Supporting Information

Minuscule weight percent of graphene oxide and reduced graphene oxide modified Ag₃PO₄: New insight into improved photocatalytic activity

Bharati Panigrahy[*] and Sachchidanand Srivastava

Solid State and Structural Chemistry Unit, Indian Institute of Science, Bangalore, 560012, India

Corresponding Author: bharatip@sscu.iisc.ernet.in

Quantum Yield Measurement using potassium ferrioxalate Actinometry[S1,S2]

The experiments were carried out in a hollow cylindrical photoreactor equipped with a water jacket. A halogen lamp (120 W, OSRAM Haloline Pro double ended halogen lamp) was used as light source in this study. Light source was positioned within the inner part of the photoreactor and cooling water was circulated through a Pyrex jacket surrounding the lamp. To study the visible light photocatalytic activity of composites, the photoreactor was encased in a UV filter (1.0M NaNO₂) which transmits only light of $\lambda > 400$ nm. An apparent quantum yield (Φ_{app}) of photocatalysts was calculated using equation

$$\Phi_{app} = \pm \frac{\left(d[x] \big/ dt \right)(mole/s)}{\left(d[h\nu]_{inc} \big/ dt \right)(Einstein/s)}$$

where, $d[x]/dt$ is change of concentration of reactant (or product) with time and $d[h\nu]_{inc}/dt$ is total numbers of photons (Einstein/s) falling on the sample. The photon flux was calculated by using potassium ferrioxalate ($K_3Fe(C_2O_4)_3 \cdot 3H_2O$) actinometry method.

The light intensity in a photochemical reactor is determined by irradiating potassium ferrioxalate ($K_3Fe(C_2O_4)_3 \cdot 3H_2O$) solution and monitoring the subsequent change in absorbance of Fe^{2+}-1,10-phenanthroline complex at 510 nm. 50 mL 3.0mM $K_3Fe(C_2O_4)_3 \cdot 3H_2O$ solution was prepared by dissolving 0.0735 gm compound in 40 mL water and 5 mL 1N H_2SO_4 in 50 mL volumetric flask and made final volume upto the mark. Ferrioxalate is a light sensitive compound and solution preparation was performed in

darkroom. For photolysis experiment, sample bottle containing 25 mL (V_1) of potassium ferrioxalate solution was exposed to photoreactor. 1.0 mL (V_2) solution was taken at different time interval (till 30 min exposure) in a 10 mL volumetric flask and mixed with 0.5 mL CH_3COONa buffer solution. 2 mL of 0.1 wt% 1,10-phenanthroline was added to this solution and made up the total volume 10 mL (V_3) by adding water. All flasks were wrapped in aluminium foil and the solution was allowed develop complex of Fe^{2+} and 1,10-phenanthroline. After one hour, the absorbance of the solutions was recorded on a UV-visible spectrophotometer at 510 nm. Fe^{2+} concentration at different time intervals was determined by standard curve obtained from Fe^{2+}-1,10-phenanthroline complex solutions.

$$\text{Light intensity (Eintsein/ s)} = \frac{\Delta n}{10^{-3}\Phi V_1 t}$$

where, Δn (moles) is ferrous ions generated after irradiation, 'Φ' is quantum yield of light used, V_1 is irradiation volume and 't' is irradiation time in second. The moles of ferrous ions (Δn) can be calculated by using

$$\Delta n = \frac{10^{-3}V_1 V_3 C_t}{V_2}$$

where, V_1 is irradiated volume (25 mL), V_2 is volume taken from the irradiated samples (1.0 mL), V_3 is volume after dilution for concentration determination (10 mL) and C_t is concentration of ferrous ions generated in irradiated solution. The concentration of Fe^{2+} (C_t) ions after dilution was determined by $FeSO_4$ calibration curve (Fig. S1). A plot of numbers of moles of ferrous ions generated vs. time was plotted and ($\Delta n/\Delta t$) was obtained from linear fit. The apparent quantum yield (Φ_{app}) of all samples was calculated at wavelength 510 nm (Φ=0.86).[S2] The photon flux (Einstein/s) of light source was calculated to be 1.77×10^{-7}.
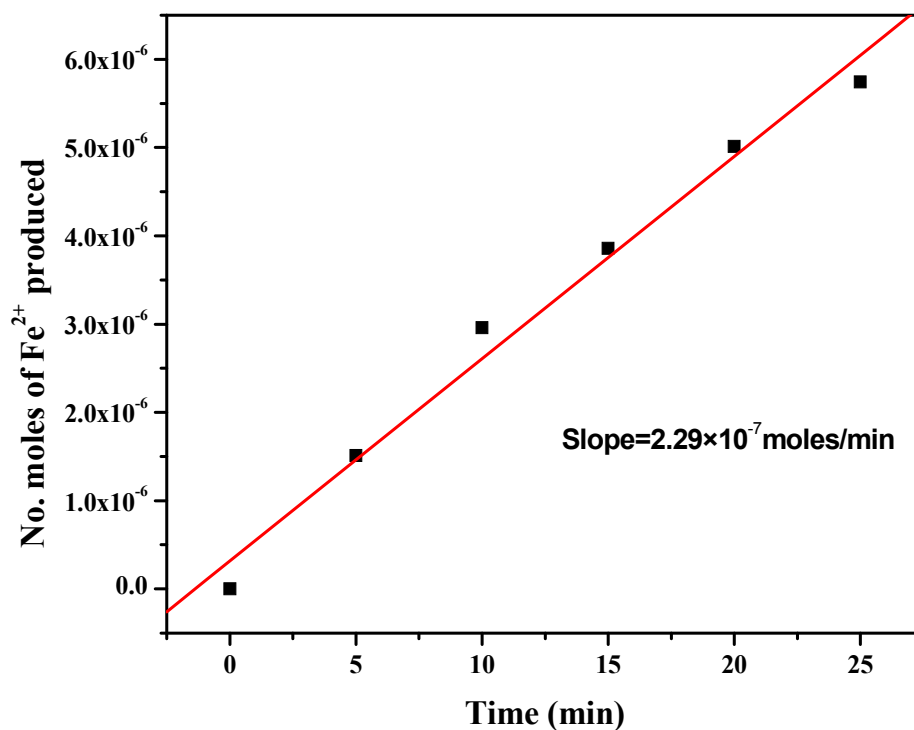
Fig. S1: Numbers of moles of Fe^{2+} ions produced after different irradiationtime exposed of visible light source.

Table S1: Apparent quantum yield (Φ_{app}) of photocatalytic degradation of RhB dye and 2-chlorophenol under visible light irradiation (at 500 nm).

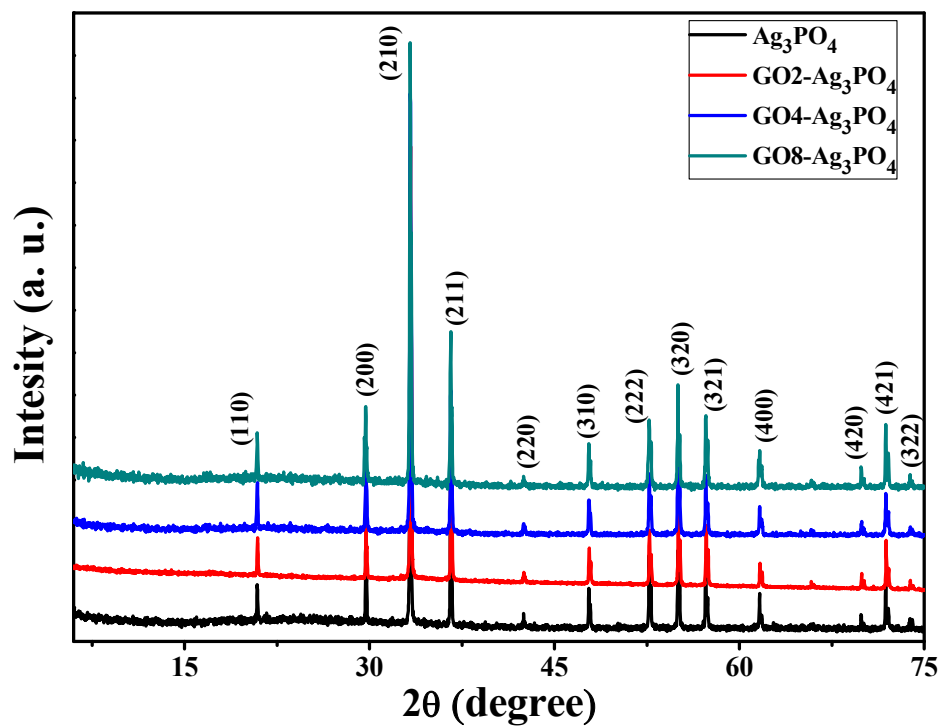| Sample	rhodamine B dye		2-chlorophenol	
	d[x]/dt (moles/s)	Quantum Yield (Φ_{app})	d[x]/dt (moles/s)	Quantum Yield (Φ_{app})
Ag_3PO_4	0.032×10^{-7}	0.018	0.087×10^{-9}	0.049×10^{-2}
$GO4-Ag_3PO_4$	0.217×10^{-7}	0.12	0.023×10^{-9}	0.013×10^{-2}
$rGO14-Ag_3PO_4$	0.045×10^{-7}	0.025	0.019×10^{-9}	0.009×10^{-2}
$rGO24-Ag_3PO_4$	0.039×10^{-7}	0.022	0.017×10^{-9}	0.0080×10^{-2}
$rGO34-Ag_3PO_4$	0.030×10^{-7}	0.017	0.0075×10^{-9}	0.0042×10^{-2}
Degussa P25	0.026×10^{-8}	0.0015	0.0015×10^{-9}	0.00084×10^{-2}

Fig. S2: Powder XRD pattern of pristine Ag_3PO_4 and GO-Ag_3PO_4 composites. All the diffraction patterns in the figure have been normalized with respect to maximum intensity peak (210).
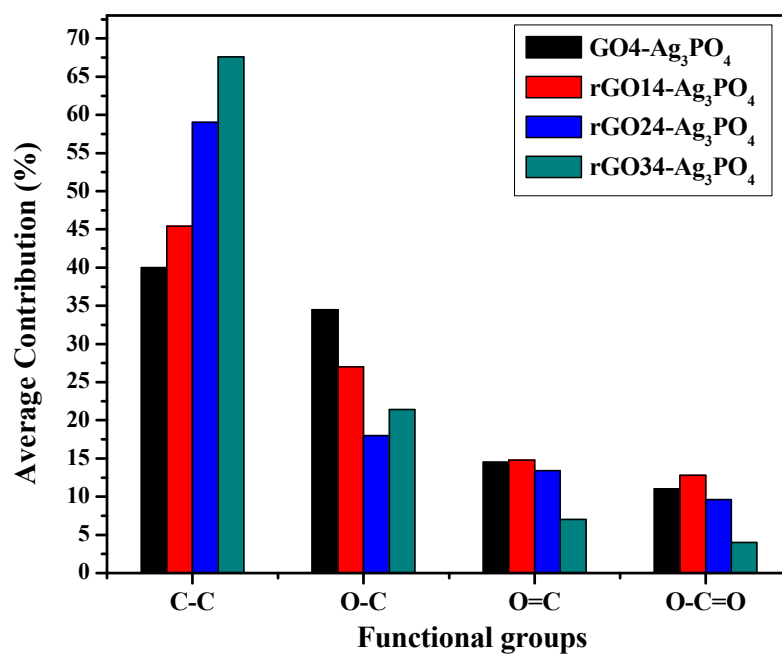
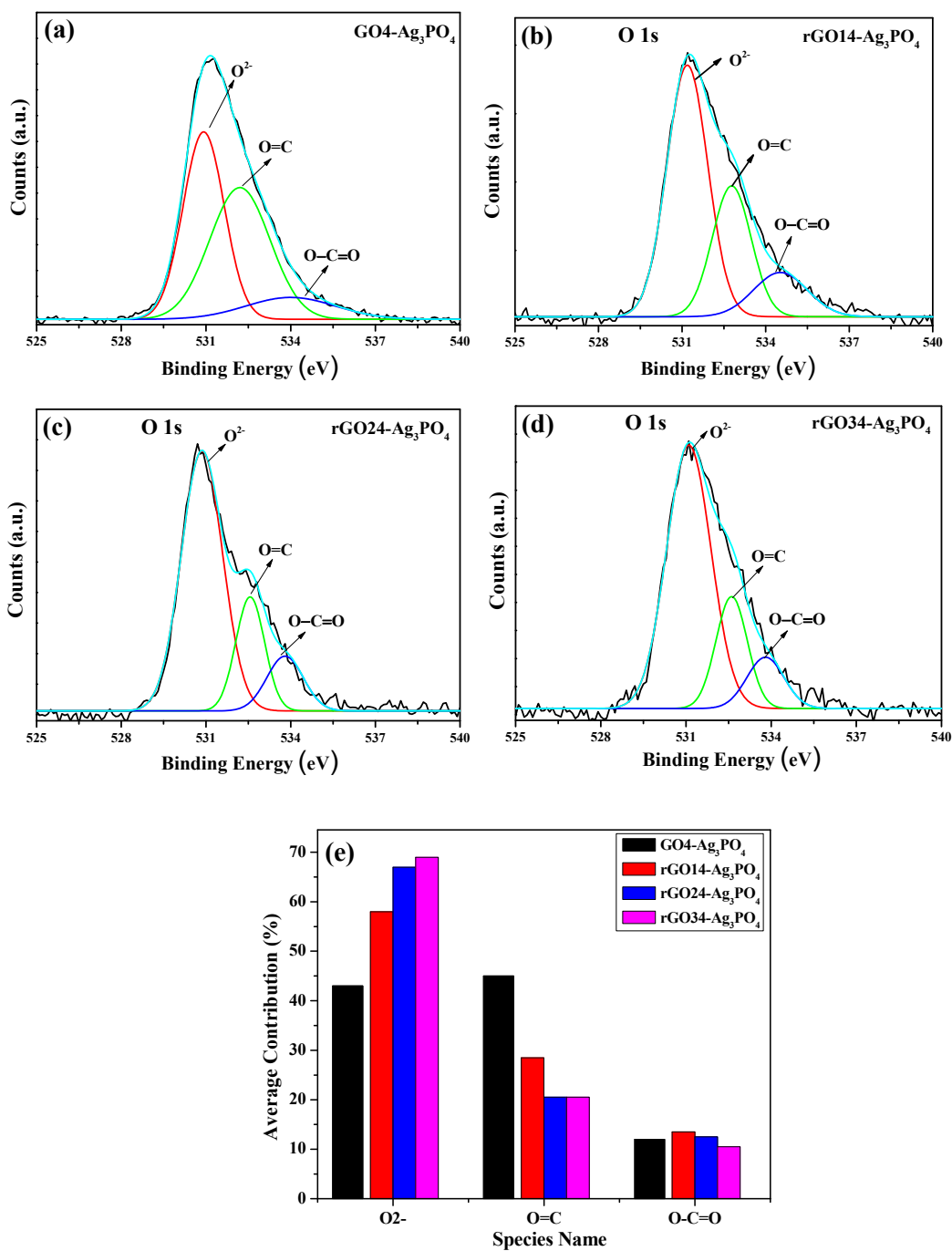**Fig. S3:** Average contribution of different species to the C 1s spectra for GO4/rGO(1-3)4-Ag₃PO₄.

Fig. S4: (a-d) High-resolution O 1s spectra of GO4 and rGO(1-3)4 modified Ag_3PO_4. (e) Average contribution of different species to the O 1s spectra.
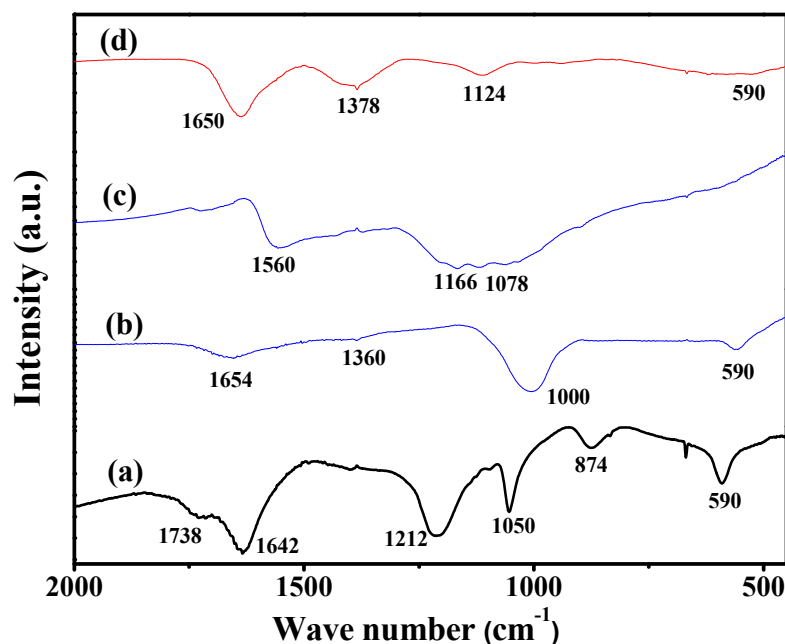
Fig. S5: FTIR spectra of (a) GO4-Ag$_3$PO$_4$, (b) rGO14-Ag$_3$PO$_4$, (c) rGO24-Ag$_3$PO$_4$ and (d) rGO34-Ag$_3$PO$_4$ composites.

FTIR spectra of GO and rGOs modified Ag$_3$PO$_4$ composites are shown in Figure S3. The FTIR spectrum of GO shows a strongabsorption band at around 1738 cm^{-1} due to the C=O stretching and 1642 cm^{-1} due to the O-H bending vibration of COOH groups situated at edges of GO sheets. It also exhibits bands around 1212 cm^{-1} and 1050 cm^{-1} due to epoxide (C-O-C) andalkoxy (C-O) groups, respectively. On the other hand, rGOs show bands at 1650 cm^{-1} and 1212 cm^{-1} which are signature of hydroxyl (O-H) and epoxy (C-O-C) functional groups attached to 2D carbon framework in rGO. The band observed around 1360-1380 cm^{-1} in all three rGOs is due stretching band of C-OH functional group. The spectra of rGO obtained from hydrazine reduction shows aromatic C=C band at 1558 cm^{-1}. It is confirmed from the reduction in the peak intensity of various functional groups that the removal of different functionalities after reducing agent treatment of GO.
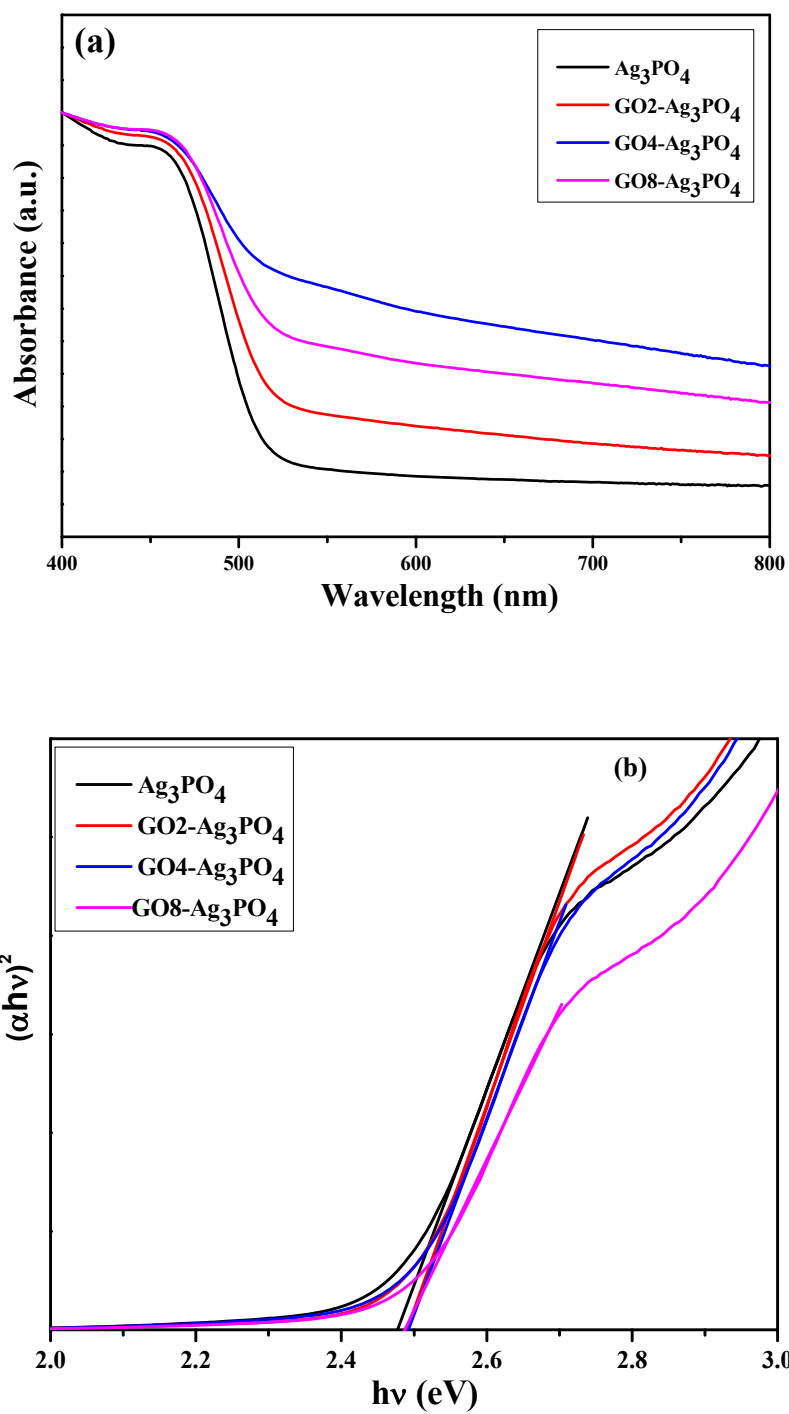
Fig. S6: (a) UV-visible diffused reflection spectra (DRS) and (b) transformed Kubelka−Munkplot of pure and different weight percentage of GO-Ag$_3$PO$_4$ composites.
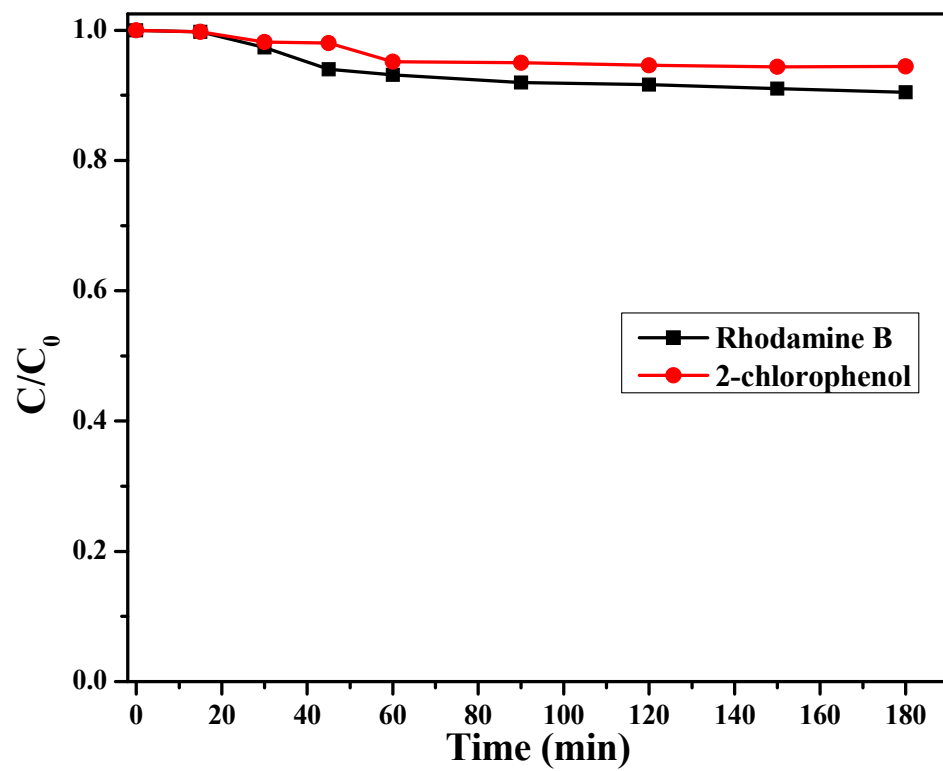
Fig. S7: Variation of absorbance of rhodamine B (RhB) and 2-chlorophol (2-CP) at different irradiation times in absence of photocatalyst.
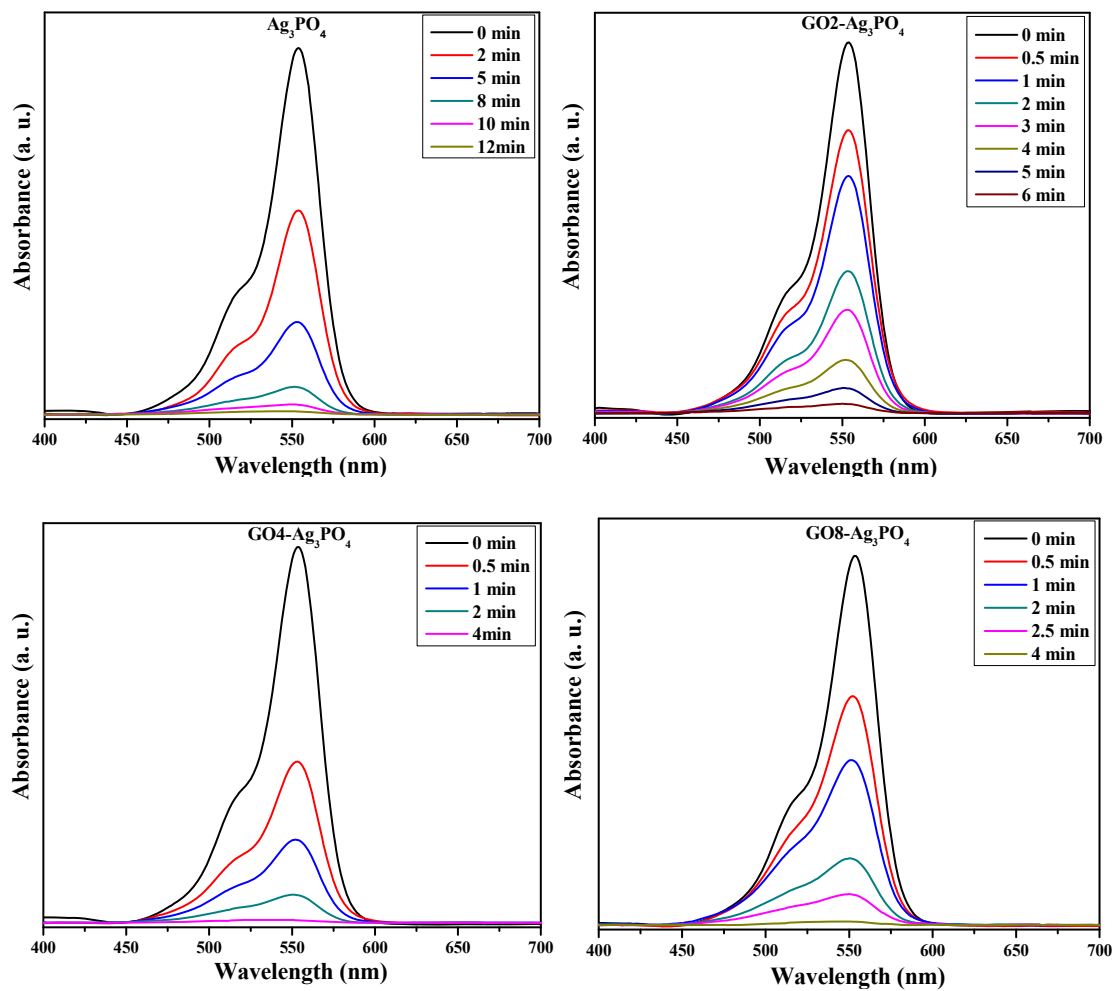
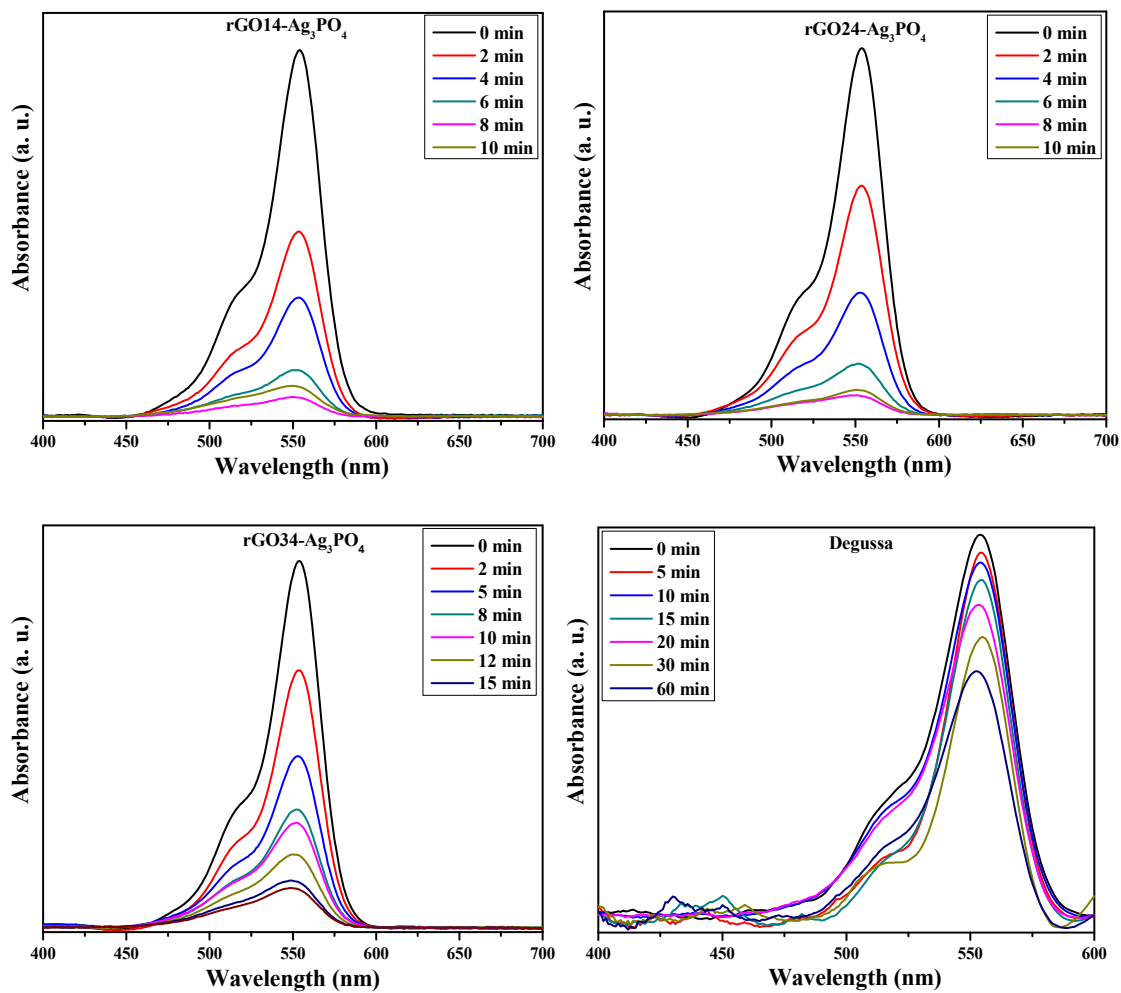**Fig. S8:** UV-visible absorption spectra of RhB dye over Ag_3PO_4 and $GO-Ag_3PO_4$ composites at different irradiation times.

Fig. S9: UV-visible absorption spectra of RhB dye over rGO(1-3)4-Ag₃PO₄ composites and standard photocatalyst Degussa at different irradiation times.
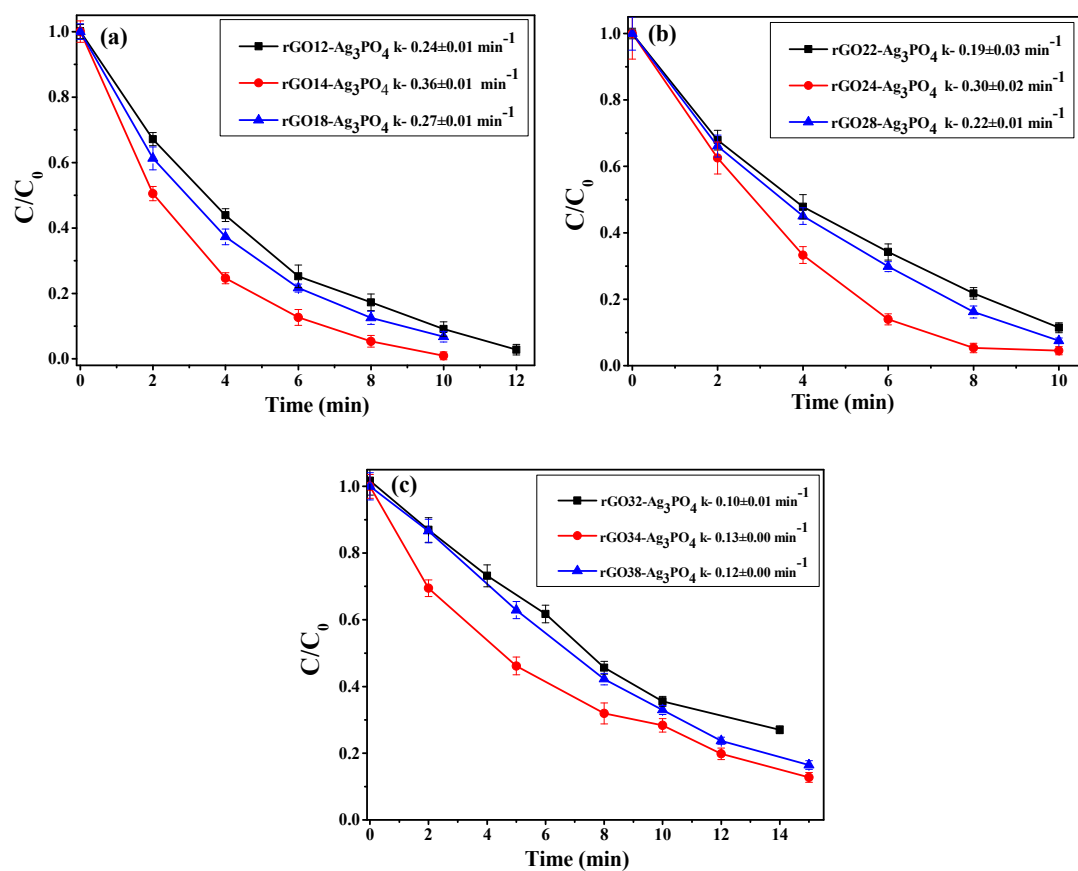
Fig. S10: Photodegradation of RhB dye as a function of illumination time for (a) rGO1-Ag$_3$PO$_4$, (b) rGO2-Ag$_3$PO$_4$ and (c) rGO3-Ag$_3$PO$_4$ composites with different rGOs concentration.
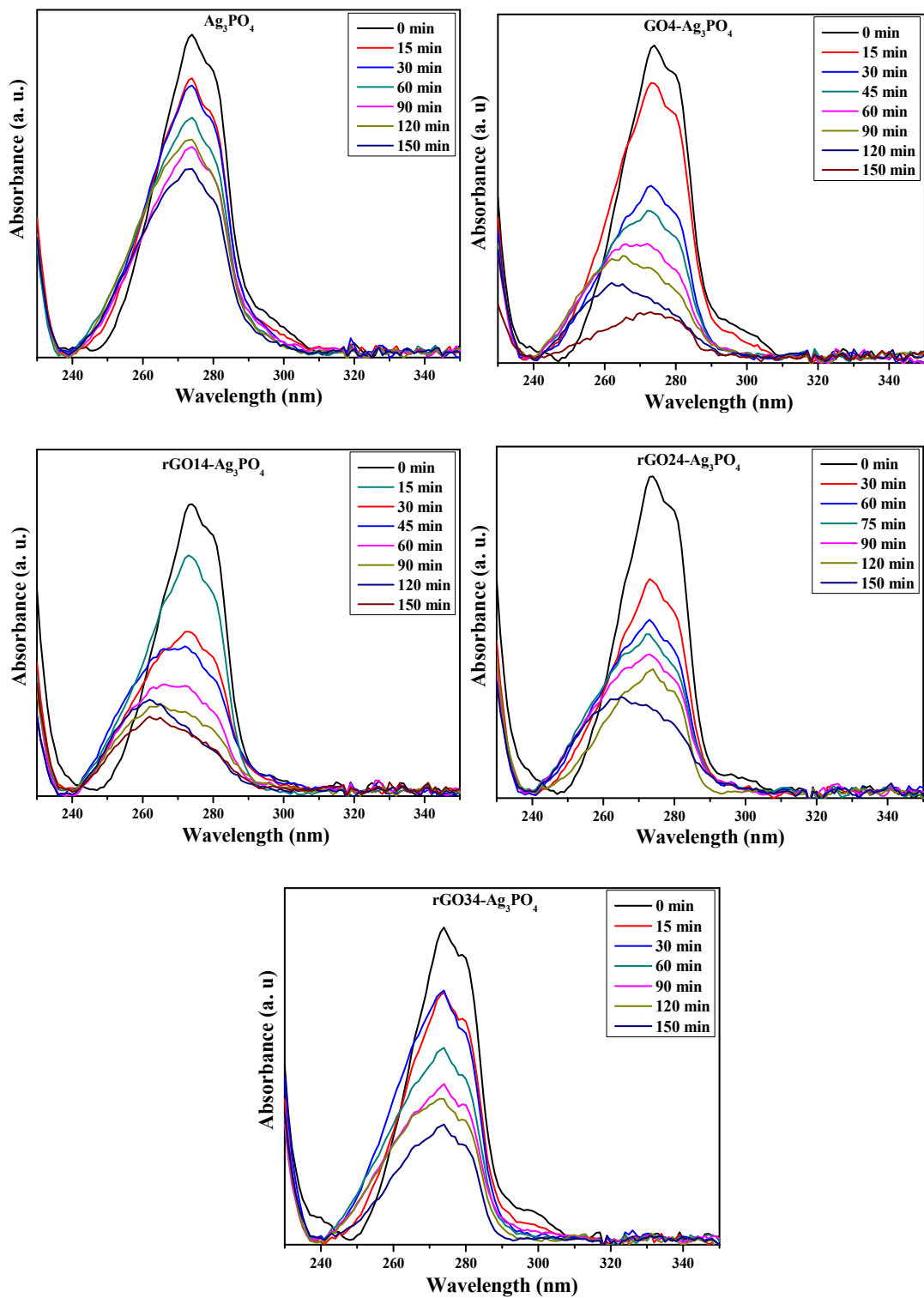
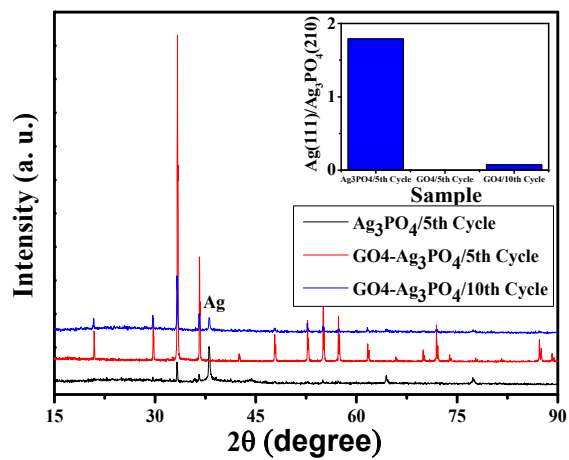**Fig. S11:** Variation of absorbance of 2-CP over GO4-Ag₃PO₄ and rGO(1-3)4-Ag₃PO₄ composites at different irradiation times.

Fig. S12: Stability studies on the photocatalytic degradation of RhB dye over (a) Ag_3PO_4 and (b) $GO4$-Ag_3PO_4 composite. (c) XRD patterns of the corresponding composites before and after recycling photocatalytic experiments.
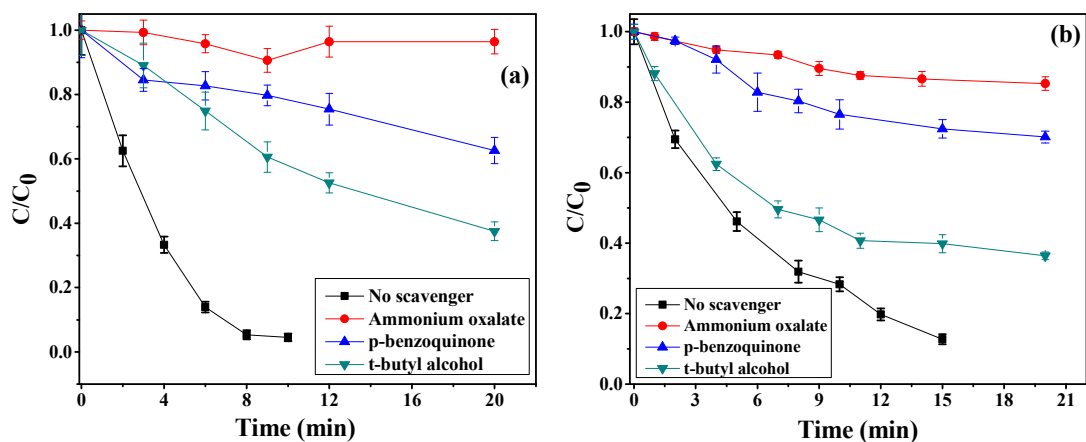
Fig. S13: Photocatalytic activities of (a) rGO24-Ag$_3$PO$_4$ and (b) rGO34-Ag$_3$PO$_4$ composites against RhB dye in the presence of different scavengers under visible-light irradiation.
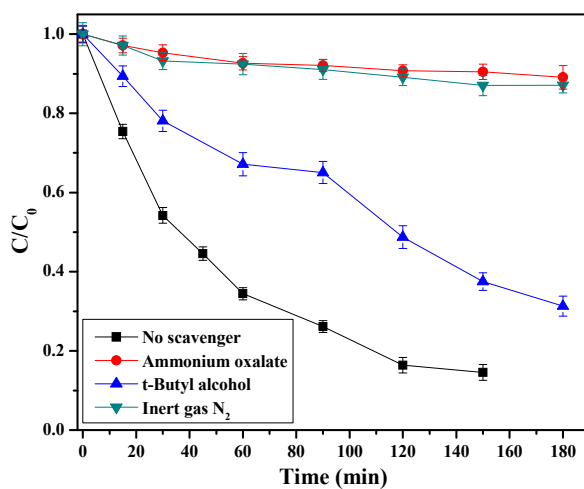

Fig. S14: Photocatalytic activities of GO4-Ag$_3$PO$_4$ composites against 2-CP in the presence of different scavengers under visible-light irradiation.

References:

[S1] J. C. Lightcap, C. Long, J. G. Vos and M. T. Pryce, J. C.Manton, C.Long, J. G.Vos, M. T.Pryce, *Dalton Trans.,* 2012, *43*, 3576-3583.

[S2] M. Montalti, A. Credi, L. Prodi and M. T. Gandolfi, Handbook of Photochemistry, Taylor & Francis, 3rdedn., 2006.